



# High-Resolution Solid-State NMR Spectroscopy of Cultural Organic Material

# 10

Joseph B. Lambert, Yuyang Wu, and Jorge A. Santiago-Blay

## Contents

Introduction .....	234
Organic Gemstones .....	235
Wood .....	240
Asphalt .....	242
Food Residues .....	242
Rubber .....	243
Lacquer .....	244
Textiles .....	245
Leather .....	246
Parchment and Paper .....	247
Bone .....	249
Paintings .....	250
References .....	251

## Abstract

Solid state NMR methods permit the examination of the bulk material of objects of importance to cultural heritage, without differential sampling characteristic of liquid- and gas-phase techniques. Solid state  $^{13}\text{C}$  and  $^1\text{H}$  methods, primarily using magic angle spinning to enhance resolution and cross polarization (only with  $^{13}\text{C}$ ) to enhance sensitivity (CP/MAS), permit analysis of organic components in a

J. B. Lambert (✉)

Department of Chemistry, Trinity University, San Antonio, TX, USA

e-mail: [jlambert@trinity.edu](mailto:jlambert@trinity.edu)

Y. Wu

Department of Chemistry, Northwestern University, Evanston, IL, USA

e-mail: [y-wu1@northwestern.edu](mailto:y-wu1@northwestern.edu)

J. A. Santiago-Blay

Department of Paleobiology, National Museum of Natural History, Washington, DC, USA

e-mail: [blayj@si.edu](mailto:blayj@si.edu)

wide variety of historical and archaeological materials, including gemstones (amber, jet), wood, asphalt, food residues, rubber, lacquer, textiles, leather, parchment, paper, bone, and paintings. Heretofore the main drawback of the technique is that sample sizes are relatively large, 50–200 mg. Recent results, however, demonstrate that the use of a small sample chamber with very high spinning speeds can permit acquisition of data on <5 mg of sample.

---

**Keywords**

Amber · asphalt · bone · jet · lacquer · leather · paintings · paper · parchment · rubber · textiles · wood

---

**Introduction**

Although nuclear magnetic resonance (NMR) spectroscopy established itself as the leading method for structural determination of materials in solution by the 1960s [1, 2], solid materials remained unapproachable at the level of high resolution because of interactions between nuclei that are not averaged by the rapid motions present in solution. In particular, dipolar and quadrupolar coupling and chemical shielding anisotropy lead to strong interactions, rapid relaxation, and broad signals. In the 1970s John S. Waugh and others developed methods involving rapid spinning of the sample to remove the effects of shielding anisotropy, along with strong irradiation to ameliorate the effects of dipolar interactions, thus achieving nearly high-resolution results, for which he was awarded the Wolf Prize in 1983/4.

Rotation is carried out at the strategic angle of  $54^{\circ}44'$ , corresponding to the angle between the edge of a cube and the adjacent solid diagonal, referred to as the magic angle, and resulting in averaging of the Cartesian axes analogous to the process of tumbling in solution [3, 4]. Such procedures are particularly effective with spin- $\frac{1}{2}$  nuclei such as  $^{13}\text{C}$ ,  $^{31}\text{P}$ , and  $^{29}\text{Si}$ , and supplemental methodologies have been developed for quadrupolar nuclei such as  $^{27}\text{Al}$  [5]. Since strong irradiation is effective only when the irradiated nucleus ( $^1\text{H}$ ) has a larger gyromagnetic ratio than and is different from the observed nucleus, these procedures fail with observation of  $^1\text{H}$ , for which specific but less effective methodologies have been developed [6]. In popular usage, the procedure of rapid rotation has been called magic angle spinning (MAS) or rotation (MAR), and the particular type of strong irradiation has been called cross polarization (CP), a process that minimizes dipolar coupling, eliminates scalar ( $J$ ) coupling, and enhances spin polarization of the low-gyromagnetic-ratio nucleus ( $^{13}\text{C}$ ,  $^{29}\text{Si}$ , etc.) by thermodynamic interaction with the high-gyromagnetic-ratio nucleus ( $^1\text{H}$ ). In this chapter, we focus primarily on the carbon nuclide and occasionally the hydrogen nuclide of organic materials, as inorganic materials, including carbonate and phosphate, are considered elsewhere in this volume by Spyros [7].

Early applications of CP/MAS procedures focused on materials of practical importance, such as coal and high polymers, but practitioners soon widened the

field to include solid organic, inorganic, and biochemical materials of all types [3, 4]. Applications to materials of importance to cultural heritage began in the early 1980s [8] and have slowly increased, limited primarily by the availability of appropriate instrumentation as well as the often valuable nature of the material being analyzed and the large sample size required. This review examines solid organic cultural materials, organized by composition. In the archaeological context, the material usually is termed an artifact; in the art and historical contexts, simply an object. We will use the latter term for generality and comprehension.

---

## Organic Gemstones

*Amber.* Although almost all gemstones are inorganic, there are at least two organic gemstones. By far the most famous such material is amber, which is produced through geological maturation, or fossilization, of plant resins. Such a process may take as long as a million years [9], with the result being the attractive, translucent, yellow/orange/red/brown material that has been used as jewelry throughout history and extending into prehistory. The material is hard and chemically robust. In contrast, resin that is incompletely fossilized may be equally attractive but is less robust. Such materials have been called *copals*.

Because amber is found throughout the world, a primary desideratum of scientific examination is to provide provenance attribution. Unfortunately, such has not proved to be the case in the general sense. Ambers from a variety of localities have been found to give very similar NMR spectra. Unlike many inorganic materials, for which characteristics such as trace element fingerprints or isotope ratios are geographically dependent, the main determinants for the NMR spectra of amber appear to be the paleobotanical origin and the extent of maturation, that is, the specific type of plant from which the original resin came and the extent of molecular alteration as the result of oxidation, polymerization, and other processes over geological periods of time.

Examination of amber from worldwide sources has identified four distinct paleobotanical compositions [10]. Baltic amber (NMR Group C), found in countries around the Baltic Sea, has a conifer source related to pines and cypresses (plant families Pinaceae and Cupressaceae) [9]. Its  $^{13}\text{C}$  NMR spectrum is dominated by a characteristic pattern of resonances from saturated carbons ( $\delta$  10–65), the presence of clear peaks at  $\delta$  110 and 150 from exomethylene unsaturated carbons ( $>\text{C}=\text{CH}_2$ ), and the carbonyl resonance of succinic acid ( $\text{HO}_2\text{CCH}_2\text{CH}_2\text{CO}_2\text{OH}$ ,  $\delta$  173) (Fig. 1, lower), from which the mineralogical name succinite derives. Closely related is a worldwide wide set of ambers (NMR Group A), also from conifer sources, mostly likely the plant family Araucariaceae, found in Europe (often with mineralogical names such as walchowite and simetite), Southwest Asia, Siberia, Japan, North America, and Greenland. The typical  $^{13}\text{C}$  spectrum of a Group A amber resembles that of Group C, but typically lacks resonances from succinic acid and exomethylene carbons (Fig. 2, of a sample from Spain). The lower spectra in the figures were

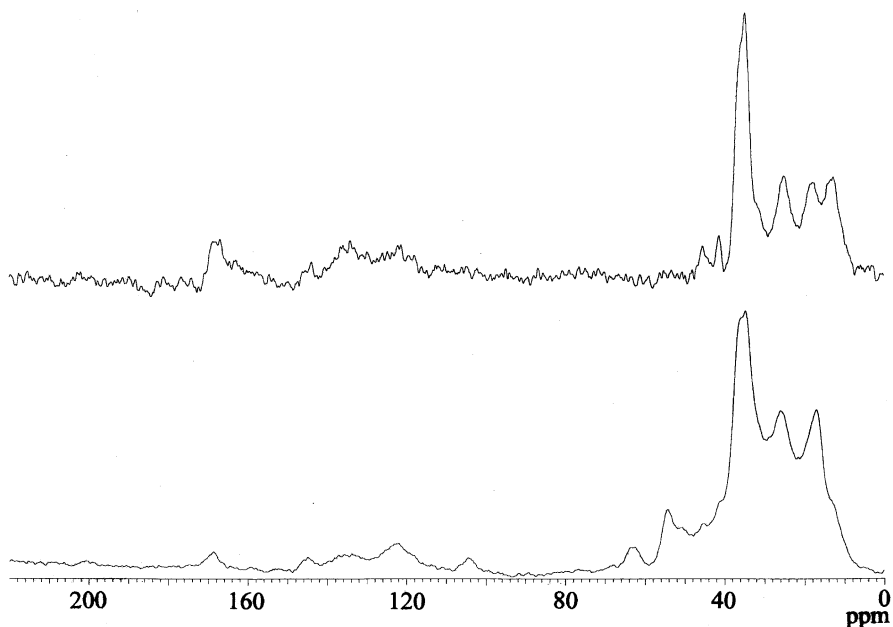


**Fig. 1** The solid state  $^{13}\text{C}$  spectrum of Baltic amber representing Group A, with (*upper*) and without dipolar dephasing

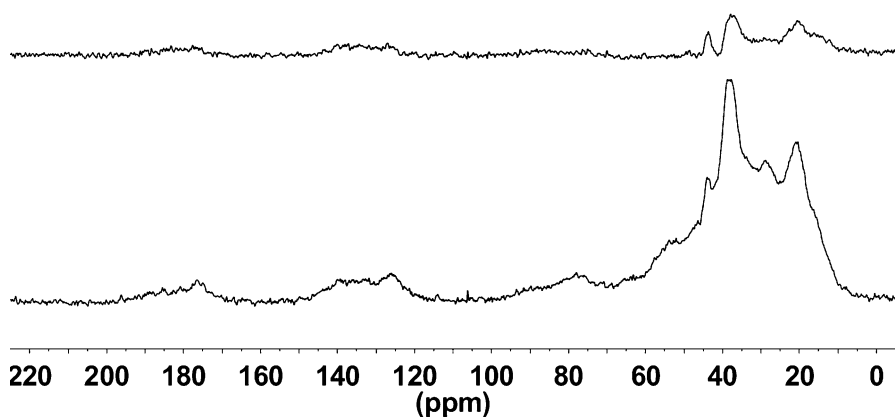


**Fig. 2** The solid state  $^{13}\text{C}$  spectrum of fossilized resin from Valdálga, Cantabria, Spain, provided by Teruhisa Ueno, Fukuoka, Japan, sample no. 1540 in the Trinity University collection, with (*upper*) and without dipolar dephasing. The humps at  $\delta$  ca. 75 and 175 are spinning sidebands of the peaks at  $\delta$  ca. 125

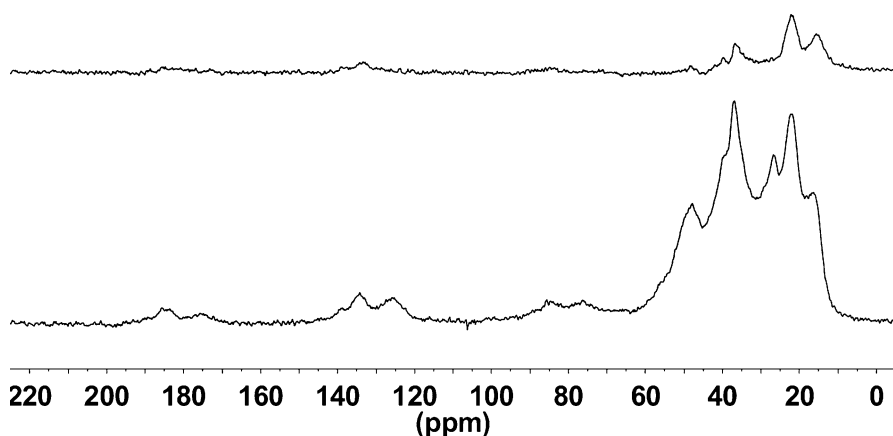


**Fig. 3** The solid state  $^{13}\text{C}$  spectrum of fossilized from South Sumatra, Indonesia, provided by Teruhisa Ueno, Fukuoka, Japan, sample no. 1537 in the Trinity collection, with (*upper*) and without dipolar dephasing

recorded with normal decoupling of all proton frequencies, whereas the upper spectra were recorded with an interruption of the decoupling (dipolar dephasing), which yields a spectrum of selected resonances, primarily quaternary carbons.

NMR Groups B and D represent amber that is derived from angiosperms or flowering plants. Group B is nearly worldwide, with concentrations in South Asia, Southeast Asia, and Japan but also the United States. It is never found in Europe, Southwest Asia, or South America. Figure 3 (a sample from Indonesia) exhibits the characteristic saturated pattern as well as a few unsaturated peaks ( $\delta$  120–140) without exomethylene resonances. These ambers have been related to the Dipterocarpaceae [11]. Group D is found in Latin America, the Caribbean, and Africa and derives from the Fabaceae or legume family [12, 13]. In addition to the characteristic saturated region, these ambers exhibit unsaturated resonances that include exomethylene groups (Fig. 4, of a sample from Uruguay). Parallel distinctions of Groups A–D have been found with proton spectra [14].

Although the four groupings of amber have overlapping geographical origins, distinctions sometimes can be made for archaeological amber. Lambert and co-workers [15] examined amber beads found in post-contact Maya burials excavated in Tipu, Belize. The beads produced Group C spectra, whereas indigenous amber would have been Group D. The beads thus were examples of Baltic amber, which presumably arrived with the Spanish. In contrast, amber found in earlier archaeological contexts (100–1000 AD) at the sites of Punta Candelero in Puerto Rico, Bayamón in Puerto Rico, and Nahuage in the Colombia state of Magdalena proved to be from Group D, the expected botanical type for Latin America [13]. The Puerto Rican samples matched particularly well with mining sites in the Dominican Republic. The Colombian samples had been heated, a process that alters the NMR spectra, which still were consistent with sources in Venezuela, the Dominican Republic, or Mexico. All these ambers clearly were not of European origin.

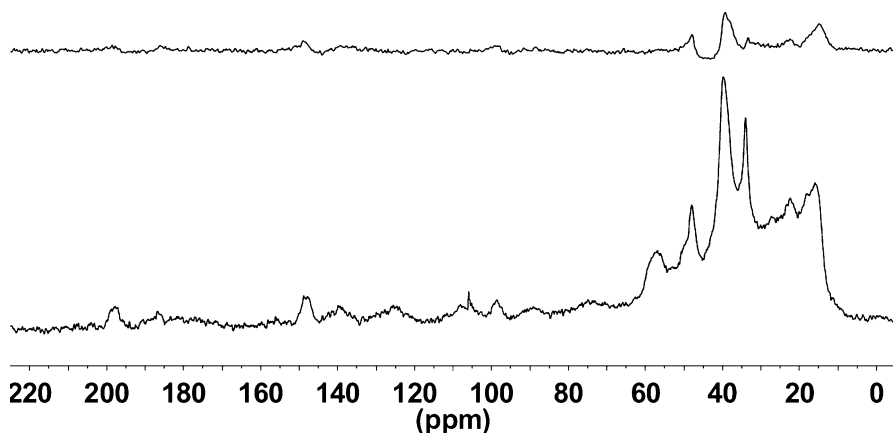


**Fig. 4** The solid state  $^{13}\text{C}$  spectrum of fossilized resin from Uruguay, provided by Crystal Triad and Patrick Craig, Guerneville, CA, sample no. 1427 in the Trinity collection, with (*upper*) and without dipolar dephasing

*Jet, Stantienite, and Oltu Stone.* The maturation of the woody part of plants can produce materials that have been valued for their shiny black appearance and used as jewelry and decorative objects. In Europe, such materials are called *jet*, a word that as an adjective refers to the deep black color. Jet is formed in the same process as coal, whereby plants are successively transformed into peat, lignite, sub-bituminous coal, bituminous coal, anthracite, and graphite by geological processes involving high temperatures and pressure over time. In terms of NMR spectroscopy, the higher ranked coals exhibit decreasing aliphatic and carbohydrate resonances and increasing alkenic and aromatic resonances. The first examination of jet by solid state  $^{13}\text{C}$  NMR spectroscopy, necessary because the material is entirely insoluble in all solvents, revealed that the coal rank is between lignites and sub-bituminous coals [16]. These materials were selected for their cleanliness to touch, in contrast with coal, and their abilities to be carved and polished, in order to achieve appropriate shapes with a high sheen. The spectra of jet from English and Spanish sources revealed similarities in the approximate equality of the saturated and unsaturated resonances (Fig. 5). Both shared distinctive phenolic peaks at  $\delta$  120 and 155. Differences were observed between the English and Spanish jets, particularly under conditions of dipolar dephasing [16]. Examination of jet samples excavated in the post-contact, Maya site of Tipu in Belize indicated they resembled Spanish jet and presumably were trade items, like the amber found at the same site [15].

Similar materials have been found in other parts of world, such as the Caribbean (Trinidad in particular) and Asia Minor (the Anatolian Peninsula in Southwest Asia). In the Baltic Sea region, such materials were termed stantienite and, in Turkey, they have been called Oltu stone, after the Turkish town of that name [17]. Oltu stone has

**Fig. 5** The solid state  $^{13}\text{C}$  spectrum of jet from Whitby, England. The peak at  $\delta$  230 is a spinning sideband

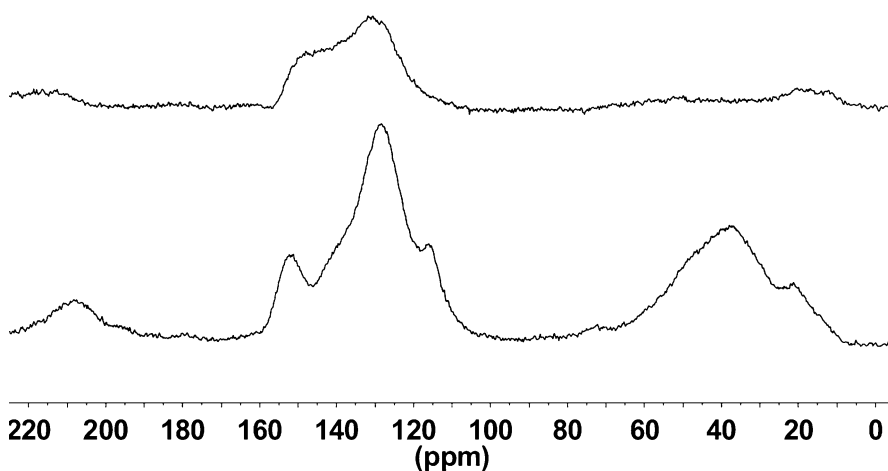
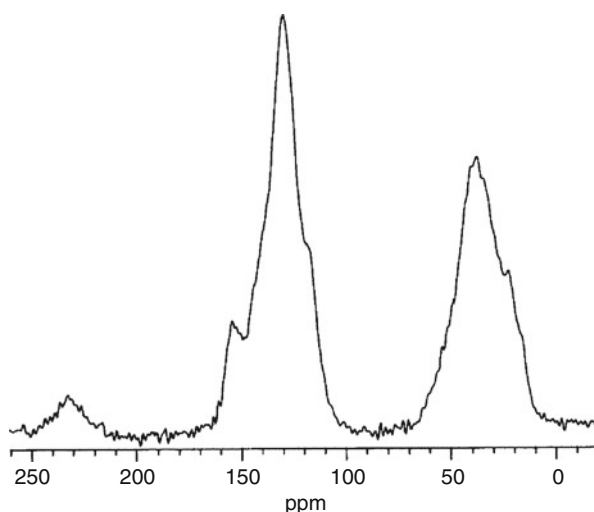
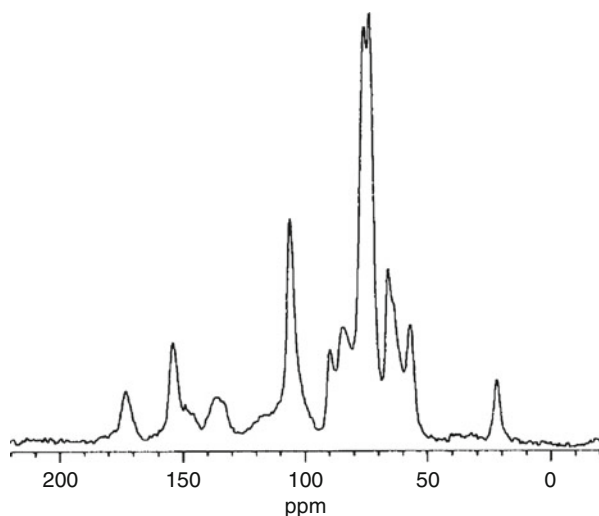


**Fig. 6** Oltu stone. The solid state  $^{13}\text{C}$  spectrum of Oltu stone from Erzurum, Turkey, provided by Serap Mutun, Abant Izzet Baysal University, Bolu, Turkey, with (*upper*) and without dipolar dephasing

been used there for decorative objects, in a similar role to jet in Europe. Interestingly, the English word *jet* derives from the Old French word *jaiet* (modern French *jais*), which in turn derives from Gagas, said to refer to a city and river in Asia Minor. The solid state  $^{13}\text{C}$  spectra of stantienite and of Oltu stone are distinctive but similar to those of jet (Fig. 6). Both materials are products of coalification but of slightly different levels of maturation.

**Fig. 7** The solid state  $^{13}\text{C}$  spectrum of drillings from the willow tree, *Salix* sp. (Reproduced with permission from Ref. [19])



## Wood

Although wood was used possibly a million years ago by early humans as a fuel, cultural functions began with its use as worked building material and as a medium for decorative objects. It is prone to rapid decomposition, but under favorable conditions can survive. The chemical makeup of wood comprises three groups of polymers: 40–45% cellulose, 20–30% hemicellulose, and 20–30% lignin. Whereas lignin is composed predominately of aromatics and alkenes, cellulose is a carbohydrate with only saturated carbons, and hemicellulose is a smaller carbohydrate. Wood is insoluble in solvents for the most part, so examination of the total content had to await the development of magic angle spinning and cross polarization methods. NMR spectra of wood as a powder contain resonances from aromatics/alkenes (from the lignin) and aliphatics (from the sugars). In their classic paper on the early application of these techniques [18], Schaefer and Stejskal at Monsanto included studies of wood and established that the technique might be able to distinguish various species, such as maple and pine. Figure 7 displays the CP/MAS spectrum of a modern willow, *Salix* sp., examined as drillings [19]. The aliphatic resonances from the sugars occur in the region  $\delta$  50–90, as almost every carbon atom is attached to an oxygen atom. In addition, the anomeric carbons, attached to two oxygen atoms, resonate at  $\delta$  105. The lignin peaks, both aromatic and alkenic, resonate in the region  $\delta$  110–160. There also is a small carboxyl resonance at  $\delta$  173, and resonances of methyl groups not attached to oxygen in the hemicelluloses component are at  $\delta$  21.

Hatcher and co-workers [20, 21] carried out early studies of ancient wood by solid state  $^{13}\text{C}$  methods. Samples from the Miocene (Poland) and the Eocene (Germany), when compared with modern samples, exhibit loss of the carbohydrate



component and preservation of the lignin. In a separate study of wood fragments buried in anaerobic sediments from 450 years ago to 8 Ma ago, they also found the steady loss of carbohydrates and retention of lignin. They interpreted the results in terms of the classical process of coalification, whereby woody tissue progresses to lignite and higher stages of coal, with the result that coal contains more of the highly condensed lignin. They characterized a Miocene sample of brown coal as having approximately 75% lignin and 25% cellulose and representing a poorly matured form of coal. Attalla and co-workers [22] carried out a more targeted study of wood from the species *Phyllocladus trichomanoides* that had been buried in a volcanic eruption in New Zealand some 200 years ago. They found that the fossilized sapwood had a greater carbohydrate content than did the fossilized heartwood from the interior of the wood, indicating differential fossilization in various parts of the wood. Although ratios of unsaturated (lignin) to saturated (carbohydrate) resonances are rough measures of the age of the wood, these studies indicate that several factors affect the results, including conditions of burial, age, and specific woody part.

Bardet et al. obtained similar results with archaeological wood from the eleventh century from Lake Paladru, Charavines, France [23], and on wood from three canoes currently undergoing conservation in Lisbon, Portugal [24]. They found complete loss of the hemicellulose signals but maintenance of the lignin signals. They also demonstrated the feasibility of obtaining good spectra on 4–6 mg of material with a microrotor with a volume of only 11  $\mu\text{L}$ .

Pournou [25] examined oak wood from a sixteenth century Greek shipwreck from near the Ionian island of Zakynthos and provided parallel information on residues of hazelnuts (from the same wreck) and olive pits (from the Macedonian site of Pella, 300 BC), grouping the artifacts as lignocellulosic materials. Near absence of the peaks at  $\delta$  ca. 20 and 173 again indicate the loss of hemicellulose, whereas maintenance of other peaks indicates the continued presence of lignins and cellulose. The two types of seeds were differentially decomposed, the hazelnuts retaining only the outer pericarp and seed coat (no seed) and the olive pits retaining the endocarp (the innermost part of the pericarp) and the seed coat. Nonetheless, all materials exhibited the similar loss of hemicellulose.

Conservation of archaeological woods often utilizes polyethylene glycol (PEG) to provide stability to the materials. Its presence can make the later analysis of  $^{13}\text{C}$  spectra difficult because of the simultaneous presence of ancient and recent organics. Bardet et al. [26] demonstrated that editing procedures can nearly eliminate the PEG signals through the choice of the contact time in the cross polarization experiment. The authors also found that archaeological wood from a seventeenth-century Italian shipwreck in the Mediterranean (*La Lomellina*) treated with PEG exhibits the same two phases (ordered and disordered) as commercial PEG and that PEG is interacting with the lignin in the archaeological materials.

Bardet and Pournou [27] in a study of fossil Miocene wood from Bükkkábrány, Hungary, reported a more nuanced view of diagenesis or fossilization. They distinguished the processes coalification (as already described, slow conversion of woody materials to lignitic aromatics through loss of carbohydrates), complete petrification

or mineralization (replacement of wood by inorganics), partial or permineralization (addition of inorganics to the woody matrix), and mummification (maintenance of micro- and macroscopic molecular components). The authors compared samples of the Bükkábrány wood with modern wood and older (Oligocene) wood from a site in the Porrentruy region of Switzerland. The Bükkábrány spectra indicated loss of carbohydrate resonances and maintenance of lignitic resonances, but microscopic examination of the materials indicated that molecular components had been largely retained, despite extensive morphological degradation. The Swiss samples exhibited more traditional degradation, by which the lignitic matrix degraded to smaller molecules, even while maintaining macroscopic morphology. The mechanistic causes of these subtle diagenetic differences are not well understood.

---

## Asphalt

Asphalt, or bitumen, is a petroleum product, either refined or found naturally. It is composed of saturated hydrocarbons, aromatics, and asphaltenes (complex mixtures of high molecular-weight aromatics and heterocycles). Like petroleum, asphalt ultimately derived from algae, diatoms, and other living matter, deposited millions of years ago and subjected to heat and pressure. Asphalts occur naturally in North America (La Brea Tar Pits in Los Angeles), Venezuela (Lake Bermudez), the Caribbean (Trinidad), South Asia (Indus Valley), and Southwest Asia (Turkey, Iraq, and the Dead Sea – known to the Romans as the Asphalt Lake). Throughout the ancient world, asphalt found many uses, including to serve as mortar between bricks, to attach pieces to statuary, to repair materials, to caulk ships, to waterproof various objects, and to embalm mummies (the Persian word for asphalt is *moom*, related to the English word *mummy*) [28, 29]. Solid state NMR methods have been used to characterize natural asphalt [30, 31], and solution NMR methods have been used to characterize archaeological asphalt [32], but to our knowledge solid state NMR methods have yet to be applied to archaeological asphalt.

---

## Food Residues

Material found on the surface of or penetrating the fabric of vessels for cooking, storage, or transport of food or drink can provide important information on diet and trade. Mass spectrometric analysis can indicate specific molecules present and can infer the type of food or beverage involved. Carbon and nitrogen isotope ratios of bone and teeth probably provide the most important information, as they refer clearly to food consumed. Solid state NMR also can yield important information, although not the identity of specific molecules. Its primary advantage is that the information refers to the bulk material, and food classes often can be identified.

Oudemans and co-workers reported the earliest study of food residues on ceramic vessels from the Roman site of Uitgeest-Groot Dorresgeest in the Netherlands [33]. Soot residues comprising polyaromatic hydrocarbons provided little useful

information. Lipids and proteins could be identified in mildly charred residues. Carbohydrate peaks could be identified in more highly charred materials, including the peak at  $\delta$  105, diagnostic for the anomeric carbon (attached to two oxygen atoms). In her thesis [34], Oudemans described the multivariate analysis of the data from all analytical methods, in which she characterized several chemotypes found in the residues: A from starch rich foods, C from protein-rich charred animal products, and D from protein rich but lipid-free foods or non-food materials (chemotype B was char from wood fire).

Canadian workers examined black residues found on plates and pots from the Kame Hills complex on Southern Indian Lake in subarctic, northern Manitoba and from “prehistoric pottery from southern Ontario” [35]. They carried out control experiments by recording the spectra of burned wild rice, tubers, pickerel, and moose fat. The spectra of the archaeological samples from Manitoba round pots and Ontario shards resembled those of meat and fish, but they lacked the anomeric carbon of carbohydrates at  $\delta$  ca. 105 found even with charred rice and tubers. Such materials either were not cooked or had disappeared over time. Residues from the Manitoba flat plates exhibited peaks at  $\delta$  30 and 65–70 attributed to fats. They concluded that the pots were used to cook fish and the plates were used for frying or possibly as fat-burning lamps. Thus NMR can distinguish types of food and assess extent of charring.

Styring et al. [36] reported a limited study, as part of a larger investigation, of the solid state  $^{13}\text{C}$  spectra of modern einkorn wheat grains, heated einkorn grains, and archaeological einkorn samples from Assiros, a Bronze Age site in Greek Macedonia, and Vaihingen an der Enz, a Neolithic site in southwest Germany. The unheated modern samples contained carbohydrate peaks almost exclusively (C—O and O—C—O). With heating at 230 °C progressively for up to 24 h, the carbohydrate peaks made way to aliphatic peaks at  $\delta$  0–50 and to unsaturated peaks predominately at  $\delta$  100–140, attributed by the authors to products from the Maillard reaction between proteins and starch to form melanoidins. The archaeological samples exhibited almost complete loss of the aliphatic signals, the spectra containing only resonances in the unsaturated region. By elemental analysis, however, the samples contained a similar amount of nitrogen to the modern samples heated for 24 h. The ancient samples thus retained amino acids in the predominantly aromatic melanoidins, which are resistant to further degradation.

---

## Rubber

Rubber is a polymer of the five-carbon monomer isopropene (2-methyl-1,3-butadiene), formed biologically in trees such as *Castilla elastica*, originally found only in Mexico, Central America, and northern South America. Indigenous people exploited its properties for at least 4000 years [37]. Artifacts extracted from water-filled sinkholes in Yucatan, called *cenotes*, include rubber balls, rubber figurines, and a stone tool hafted with a rubber band. The Nahuatl name for the Olmecs of southwest Mexico, who were responsible for the earliest major

civilization in Mexico, *olmecatl* came from the two Olmec words *olli* (rubber) and *mecatl* (people), so the Aztecs called them “the rubber people.” Hosler et al. in 1999 reported analysis by solid state  $^{13}\text{C}$  NMR spectroscopy of a cache of rubber balls found at the Olmec site of Manatí in the Mexican state of Veracruz, with dates in the range 1600–1200 BC [38]. The balls were used in the ancient religious and sporting activity called *pelota* by the Spanish, for which ball courts have been found all over Mesoamerica and some Caribbean islands. Such polymers are insoluble and consequently could be studied only by solid state methods. The authors found the characteristic five-carbon spectrum of *cis*-polyisopropene in the Olmec balls as well as in the spectra of pure modern rubber latex.

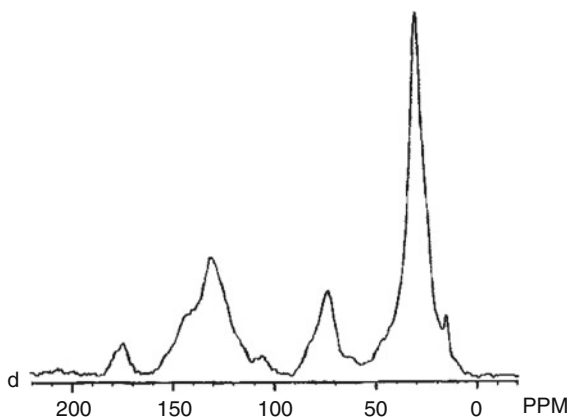
The rubber from pure rubber latex becomes brittle over time. It has been known since the time of the *conquistadores* that the Mesoamerica rubber ball was produced by heating latex from the rubber tree with a small amount of the juice from the morning glory vine (*Ipomoea alba*), which conveniently grows on the rubber tree. Thus the Olmecs and their cultural descendants were engaged in chemical manufacturing, without which the important cultural activity of the ball game could not have developed. Hosler et al. further found that unprocessed modern latex gives spectra with peaks not found in the ancient rubber, indicating that there was an element of purification in the ancient process. They further hypothesized that the morning glory juice encouraged cross-linking or chain entanglement, which would increase elasticity and reduce brittleness.

---

## Lacquer

Like rubber and amber, oriental lacquer is a product derived from a plant exudate. Also like rubber, it requires processing by humans in order to create the material of cultural importance. The hard, easily polished product has been known for 4000 years in China. It resists analysis because of its extreme insolubility. The plant exudate (raw lacquer) contains 20–25% water, 10% carbohydrates, and 65–70% urushiol. Urushiol also is the active ingredient in poison ivy, poison oak, and poison sumac. Urushiols all are *ortho*-dihydroxybenzenes (catechols) with a third substituent on the benzene ring, a hydrocarbon chain of variable length. The various allergens differ from each other and from the sap of the lacquer tree (*Toxicodendron vernicifluum*, formerly *Rhus vernicifera*) in the length of the hydrocarbon chain and the extent of unsaturation. The curing process brings about oxidation and, particularly, polymerization, by which the phenolic functionalities condense with the side-chain double bonds. Lambert et al. [39] examined four samples of modern Chinese and Japanese lacquer by solid state carbon NMR methods. The spectra (Fig. 8) exhibited expected aromatic resonances from the catecholic structures and alkenic resonances from the unsaturations in the side chains in the region  $\delta$  100–160, saturated resonances from the methylene and methyl groups in the side chains at  $\delta$  20–50, small carboxy resonances at  $\delta$  175 presumably from oxidation products, and a resonance at  $\delta$  75. This last resonance corresponds to structures containing a

**Fig. 8** The solid state  $^{13}\text{C}$  NMR spectrum of the black portion of a Japanese sample of lacquer. (Reproduced with permission from Ref. [39])



saturated C—O bond. Raw urushiol lacks such a structure, which is formed on condensation of the phenolic groups with the unsaturated side chains. The peak thus confirms the mechanism of polymerization and provides a measure of the extent of polymerization. The Chinese sample, for example, exhibited a smaller resonance at  $\delta$  75 than the Japanese samples. The result may not be general, because there was only a single sample from China.

## Textiles

The term *textile* refers to any manmade network of spun fibers, including both plant fibers such as cotton and linen and animal fibers such as wool and silk. Such materials date back at least 30,000 years [40]. Because of the high potential for degradation under archaeological conditions, surviving textiles normally are too precious to submit to the conditions for  $^{13}\text{C}$  NMR solid state analysis. A few studies of historical materials have been carried out, but for the most part this technique has been applied to modern materials of no commercial value.

The term cotton refers to the plant (various species of the genus *Gossypium*), the fiber, and the fabric. It consists almost entirely of the plant polymer cellulose, a polysaccharide composed of linked glucose units. There apparently were independent domestications of cotton in the Old and New Worlds: in Mexico by about 3000 BC and in the Indus River Valley possibly as early as 1000 BC, although in both hemispheres cotton fabrics from wild species were produced at earlier dates [41]. Adebajo and Frost [42] examined by solid state  $^{13}\text{C}$  methods the structural effects of acetylation of commercial cotton to improve its absorbant properties.

More relevant to conservation science, Princi and co-workers [43] examined the structural effects of in situ polymerization on the strength of degraded textiles. Natural aging produces carboxyl and other carbonyl functionalities, which provide a locus for copolymerization with acrylate monomers. The experiments were carried out on both naturally and artificially aged cotton. Aging could be simulated by

treatment of cotton with iodate to produce carboxyl groups. Cross-linking of the copolymer, it was hoped, would enhance mechanical strength and thermal stability. The authors used solid state  $^{13}\text{C}$  NMR methods to assess the degree of grafting.

Taylor et al. [44] examined cotton fiber from *G. barbadense* using solid state MAS spectroscopy for both  $^1\text{H}$  and  $^{13}\text{C}$  in order to understand the dynamics of the interactions between water and the cellulose matrix. Moisture content influences the strength of the fiber, the speed the fiber can be spun into yarn, and even the perception of comfort of the fabric to the wearer. The authors used  $^1\text{H}$  experiments primarily to assess relaxation effects. They found a range of relaxation times, including distinct responses from relatively free water and water within the cellulose. Combined  $^1\text{H}/^{13}\text{C}$  experiments indicated that the cellulose carbons are correlated with the broader water peak, confirming its assignment to the water molecules within the polymer. Such experiments would be useful with historical fabrics, to determine the extent and range of water content over time.

Linen is derived from flax fibers of the plant *Linum usitatissimum*, known for at least 30,000 years and developed to an industrial stage in Mesopotamia and Egypt more than 4000 years ago [40]. It has the reputation to be an upscale fabric, more expensive to manufacture than cotton, used for table and bed coverings, undergarments, and clothing in general. Princi and co-workers [43] included linen samples in their investigation of cross-linking to enhance fabric strength and stability.

Textiles from animal fibers include primarily wool and silk. Wool has been produced from numerous animals, such as goats, sheep, camelids (camel, alpaca, etc.), rabbits (angora), and muskoxen. Solid state NMR studies to our knowledge have been restricted to modern wool samples [45] and not to historical or archaeological samples. Silk, originally an exotic material to the Western world, is produced for the most part from fibers exuded by the Bombyx silkworm larvae (*Bombyx mori*). The fibers themselves have been studied extensively by solid state NMR methods [46], most commonly on the spider silk itself [47]. Archaeological silk has been examined by Chûiô et al. from twelfth-century mummy wrappings from members of the Fujiwara clan in Hiraizumi in northeastern Japan [48, 49]. The carbonyl (amide) region at  $\delta$  170 from fibroin molecules enabled the authors to estimate proportions of specific amino acids, such as glycine and alanine, and to draw conclusions regarding the secondary structure (anti-parallel  $\beta$  sheets).

---

## Leather

For millennia, humans have been treating animal hides to avoid brittleness, particularly with infusions of tannin-rich bark. In the archaeological context, leather is subject to decomposition and often is too precious for examination by NMR. Bardet et al. [50] examined the soles of shoes found in the excavation of an area intended for a parking lot in the St-Georges area of Lyon, France. The rich site provided leather from the soles of shoes dating from the thirteenth to the eighteenth century. They established the pattern expected for the solid state  $^{13}\text{C}$  spectra of modern leather, tanned with vegetable tannins and lubricated. Resonances of the amino acid side

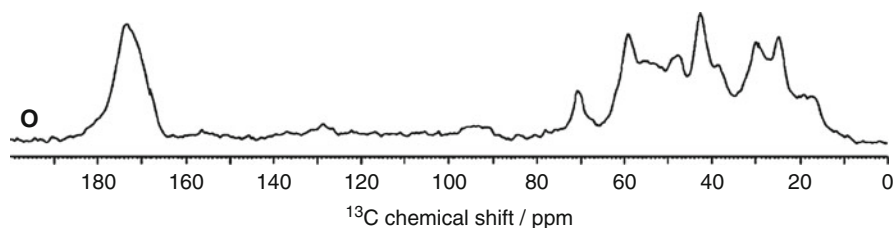


**Fig. 9** The CP-MAS  $^{13}\text{C}$  spectrum of waterlogged leather from the thirteenth century, from Lyon, France (Reproduced from Ref. [50])

chains of collagen from the hide appear in the region  $\delta$  15–75, and those from the aromatic tannin residues in the region  $\delta$  80–160. In addition, there is a single broad carbonyl band at  $\delta$  175. The archaeological samples exhibited consistent spectra that contained the carbonyl resonance and the collagen resonance but entirely lacked aromatic resonances from tannins (Fig. 9). Either the tannins had leached out or the material had not been tanned. The authors preferred the leaching hypothesis. A similar spectrum of leather from an Egyptian site (Antinoe) from an unpublished project was reported in the review by Capitani et al. [51]. Bardet et al. [50] also examined mobile domains within the materials with selectively edited spectra by combining the MAS method either with single pulse excitation (SP/MAS) or with distortionless enhancement with polarization transfer (DEPT/MAS). Although these experiments provided no significant additional information, they suggest possible directions for many other types of culturally important materials.

Popescu et al. [52] examined the wide-line, solid state  $^1\text{H}$  spectra of historical leather samples from the fifteenth to the seventeenth century from Romania. Primarily, the authors could assess water mobility. Historic leathers should have lower mobility and larger linewidths than do modern leather. One leather sample exhibited NMR patterns similar to those of parchment rather than leather, leading the authors to suggest that age-related cross-linking had transformed the leather into a material resembling parchment.

---

## Parchment and Paper

The use of animal hides as a writing surface goes back at least to the Egyptian Old Kingdom, but its processed form as parchment dates about to the second century BC to the Greek city of Pergamon, located in western Turkey, from which the word *parchment* derives [53]. Hides of goat, calf, or sheep are unhaired, limed, and dried under tension but not tanned.

Aliiev [54] examined 18 historical parchments, mostly undated but one as early as the seventeenth century, and compared the results with two recent parchments. From wide-line  $^1\text{H}$  experiments, the water content was found to decrease with the age of the sample as the result of partial hydrolysis of peptide bonds in the collagen. The water

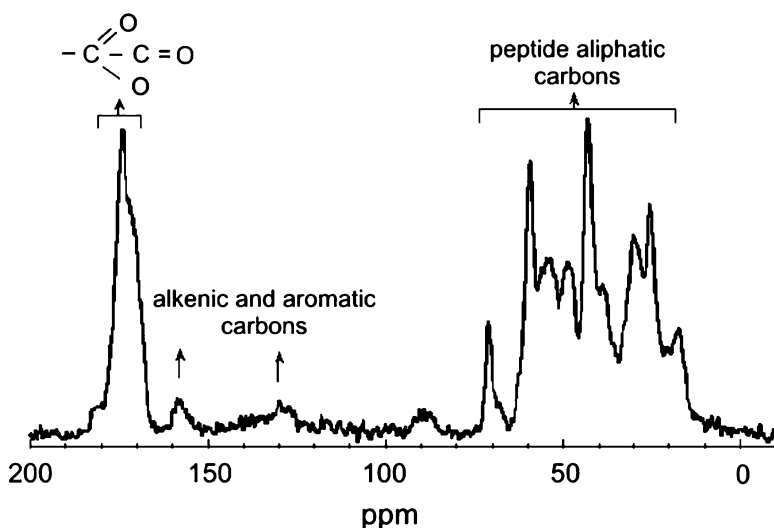


**Fig. 10** The  $^{13}\text{C}$  CP/MAS of a modern parchment (Reproduced with permission from Ref. [55])

content correlated linearly with  $^{13}\text{C}$  MAS linewidths, indicating that structural water molecules stabilize the collagen structures. From linewidth ratios, the author proposed a disordered ranking parameter that likely is related to the extent of degradation. Odlyha et al. [55] used solid state  $^{13}\text{C}$  NMR methods peripherally in their study of modern and historical parchments, mostly from Denmark, to identify and quantify the amino acid residues in the polypeptide chains (Fig. 10). Popescu et al. [52] included one historic parchment in their study, a seventeenth century religious book from Romania. The solid state  $^1\text{H}$  spectra indicated lower water mobility compared with modern sheep and kid parchments. The characteristics of the historic parchment were consistent with sheep skin.

In contrast to parchment, paper is a plant product, composed of pressed fibers of cellulose pulp from wood, rags, or grasses. Cellulose is a polysaccharide that is largely insoluble in organic solvents and water. Bastone et al. [56] used solid state  $^{13}\text{C}$  NMR methods to examine the structure of paper in a sixteenth century book. The objective of their analysis was to assess the need for conservation and to define the necessary approach. The authors included assessment of the degradation of two parchment samples taken from the cover of the book.

Corsaro et al. [57] have demonstrated, with the use of a 700 MHz NMR spectrometer, that high resolution  $^1\text{H}$  spectra of solids, both 1D and 2D, can provide important information on delicate materials of cultural importance, providing a direction for many possible applications. They examined small pieces of paper from fifteenth century Perpignan, France, and Milan, Italy. These samples came from the end leaves, carried no printing, and had already been examined in previous studies. Their spectra identified the major collagen degradation products, including



choline and hexanoic acid, as well as minor products such as pyruvic acid, the likely products of the degradation of cellulose to cellobiose and thence to smaller molecules. COSY spectra were particularly useful in identifying the peaks of lactic acid and TOCSY spectra the presence of adipic acid. The authors also identified peaks they attributed to several common amino acids, which may imply the use of animal products such as gelatin in the manufacture process. The ability to obtain the high resolution  $^1\text{H}$  spectra from archaeological and historical solids and to identify specific small molecules will permit new approaches to many other types of materials.

---

## Bone

Calcium hydroxyapatite constitutes the inorganic structural material of bone, which also contains the elastic protein collagen to improve fracture resistance. Solid state NMR methods have been applied to bone from the biomedical perspective for many years [58–61]. Lee et al. [62] examined a 15,000 year old fossil bone from Riera Cave in Spain by these methods. X-ray diffraction (XRD) demonstrated the presence of calcium phosphate hydrate, calcite, and very small amounts of hydroxyapatite, but XRD cannot detect organic material. The  $^{13}\text{C}$  solid state CP/MAS spectrum contained the calcite peak at  $\delta$  168 and broad peaks in the range  $\delta$  0–60 presumably from collagen peptide side chains. Although the authors said that the latter peaks were present “in very small quantities,” the apparent integral of the peaks exceeded that of the calcite peak, although relaxation differences vitiate any direct comparison. Thus NMR can detect organic residues in extremely old bone. The authors also performed  $^1\text{H}$  MAS experiments, which yielded apparent peaks from hydroxyl and from organics.

Alfano et al. [63] used  $^1\text{H}$  and  $^{13}\text{C}$  solid state spectra to similar effect to assess the process of diagenesis on one tooth and four bone samples from Poseidonia (Paestum), Italy, dating from the seventh century BC to the second century AD. Their progressive procedure for cleaning included physical abrasion, pulverization, drying, oxidation with hypochlorite, and treatment with acetic acid. Like Lee et al. [62], they found strong signals from remnant organic materials from collagen. In the  $^{13}\text{C}$  spectra, the carbonyl region contained two peaks of similar intensity, attributed to diagenetic calcite at  $\delta$  170, which disappeared after acid treatment, and to collagen carbonyl and structural carbonate at  $\delta$  174, which remained after acid treatment (Fig. 11).

Selasse et al. [64] reported a similar study of bone cleaning procedures, comparing treatment with 0.1 M and 1 M acetic acid, using ten samples with different preservation states from the Catacombs of Saints Peter and Marcellinus (first to third century AD Rome) and the cemetery of St. Benedict (Eighteenth century AD Prague). Exogenous carbonate was removed differently by the two techniques. Turcu et al. [65] reported MAS  $^1\text{H}$  studies of 2000-year-old bone from archaeological sites from highland Transylvania, Romania, and failed to find signals attributable to collagen.

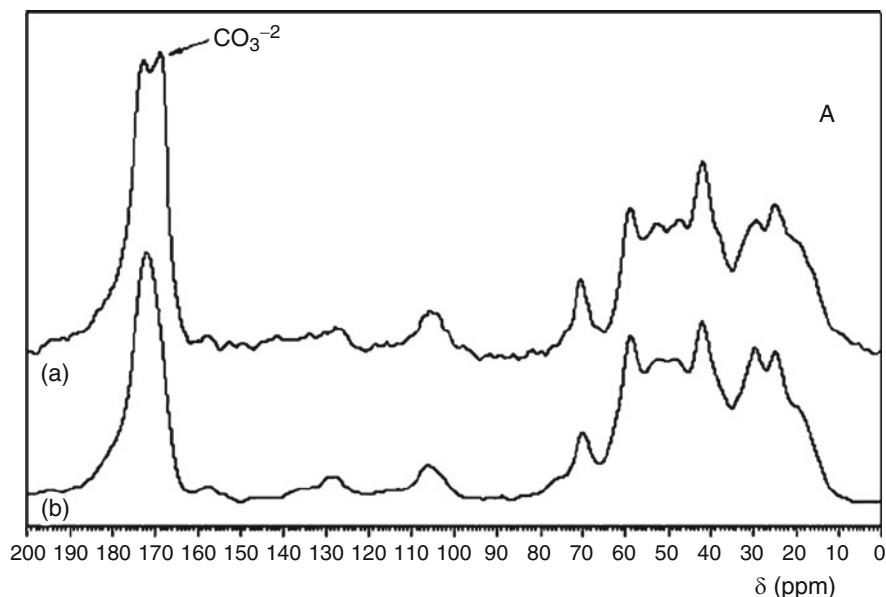
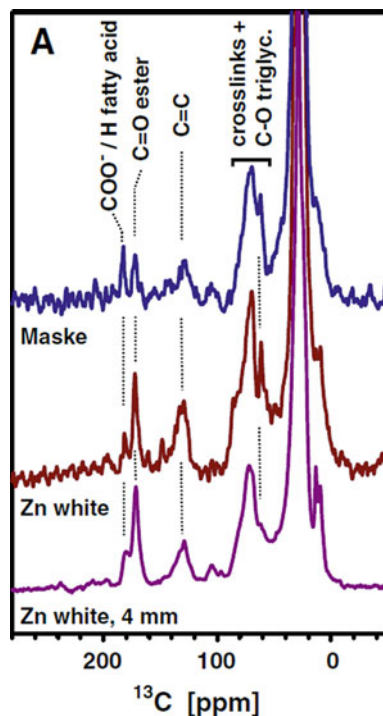


**Fig. 11** The  $^{13}\text{C}$  CP/MAS spectrum of bone from a tomb dated to the first to second century AD at Poseidonia, Italy, (a) untreated and (b) after treatment with acetic acid (Reproduced with permission from Ref. [63])

## Paintings

Unilateral NMR methods have been used extensively in the examination of paintings [66], but traditional solid state NMR spectroscopy has not been useful because it requires a sample of  $>50$  mg, prohibitive in the study of precious materials with limited sampling opportunities. Kehlet et al. [67] recently have demonstrated the ability to use a smaller sample chamber (1.3 mm rather than the standard 4 mm) and obtained results on a sample weighing only 4.7 mg from the 1945 oil painting *Maske* by Danish, avant-garde artist Asger Jorn. The study object was a small yellow flake that had become dislodged from the eye region of the figure. X-ray fluorescence analysis of the flake indicated the presence of cadmium and zinc and suggested that the pigment was a mixture of cadmium yellow and zinc white. Consequently, the authors included examination of a sample of zinc white as a reference material. As the Jorn sample weighed  $<5$  mg, data acquisition required 87 h and a very rapid rotor speed of 40 kHz (MAS normally is 3–5 kHz). The field strength was 75 MHz for  $^{13}\text{C}$  (300 MHz for  $^1\text{H}$ ); shorter acquisition times should be available from higher field instrumentation. The resulting CP/MAS  $^{13}\text{C}$  spectrum (Fig. 12) indicated that the major organic material resembled linseed oil, as represented by resonances for triglycerides and fatty acids, also present in the reference zinc white. The carbonyl resonances indicate that about half the esters had hydrolyzed to the carboxylate ion.

**Fig. 12** The  $^{13}\text{C}$  CP/MAS spectrum of (*top*) a yellow flake from the painting *Maske* by Asger Jorn and (*center and bottom*) samples of zinc white (Reproduced with permission from Ref. [67])



The authors also obtained  $T_2$ -filtered  $^1\text{H}$  spectra with ultra-high spinning speeds of 60 kHz. The resulting spectra are expected to be of the mobile fraction of the oil paint, consisting of molecules that are not cross-linked, possibly acting as a plasticizer. Comparison of the Jorn sample with the reference sample indicates less mobile fraction in the former. These results confirmed those of Bardet et al. [23] and demonstrated that solid state NMR spectra in the future can be obtained successfully with much smaller samples and less intrusive sampling of the art object than has been previously possible.

The authors thank the Welch Foundation (Departmental Grant No. W-0031), the Camille and Henry Dreyfus Senior Scientist Mentor Program, and The Pennsylvania State University, York Campus for financial support of this work.

## References

1. Lambert JB, Mazzola EP. Nuclear magnetic resonance: an introduction to principles, applications, and experimental methods. Upper Saddle River: Pearson Education, Inc.; 2004.
2. Günther H. NMR spectroscopy: basic principles, concepts, and applications in chemistry. 2nd ed. Chichester: Wiley; 1996.
3. Fyfe CA. Solid state NMR for chemists. Guelph: C.F.C. Press; 1983.
4. Duer MJ. Introduction to solid-state NMR spectroscopy. Oxford, UK: Blackwell; 2004.

5. Frydman L, Hardwood JS. Isotropic spectra of half-integer quadrupolar spins from bidimensional magic-angle spinning NMR. *J Am Chem Soc.* 1995;117:5367–8.
6. Schanda P, Meier BH, Ernst M. Quantitative analysis of protein backbone dynamics in microcrystalline ubiquitin by solid-state NMR spectroscopy. *J Am Chem Soc.* 2010;132:15957–67.
7. Spyros A. Liquid-state NMR in cultural heritage and archaeological sciences. In: *Modern magnetic resonance*. 2nd ed. Switzerland: Springer International Publishing; 2017.
8. Lambert JB, Frye JS. Carbon functionalities in amber. *Science.* 1982;217:55–7.
9. Langenheim JH. *Plant resins: chemistry, evolution, ecology, and ethnobotany*. Portland: Timber Press; 2003.
10. Lambert B, Santiago-Blay JA, Anderson KB. Chemical signatures of fossilized resins and recent plant exudates. *Angew Chem Int Ed Engl.* 2008;47:9608–16. *Angew Chem*, 120:9750–9760.
11. Lambert JB, Levy AJ, Santiago-Blay JA, Wu Y. Nuclear magnetic resonance (NMR) characterization of Indonesian amber. *Life: Excitement Biol.* 2013;1:136–55.
12. Martínez-Richa A, Vera-Graziano R, Rivera A, Joseph-Nathan P. A solid-state Carbon-13 NMR analysis of ambers. *Polymer.* 2000;41:743–50.
13. Lambert JB, Santiago-Blay JA, Rodríguez Ramos R, Wu Y, Levy AJ. Implications of nuclear magnetic resonance spectra of fossilized semi-fossilized, and modern resins from the Caribbean Basin and surrounding regions for possible pre-Columbian trans-Caribbean cultural contacts. *Life: Excitement Biol.* 2014;2:180–209.
14. Lambert JB, Tsai CY-h, Shah MC, Hurlley AE, Santiago-Blay JA. Distinguishing amber classes by proton magnetic resonance spectroscopy. *Archaeometry.* 2012;54:332–48.
15. Lambert JB, Graham EA, Smith MT, Frye JS. Amber and Jet from Tipu, Belize. *Ancient Mesoamerica.* 1994;5:55–60.
16. Lambert JB, Frye JS, Jurkiewicz A. The provenance and coal rank of jet by Carbon-13 nuclear magnetic resonance spectroscopy. *Archaeometry.* 1992;34:121–8.
17. Lambert JB, Santiago-Blay JA, Wu Y, Levy AJ. The structure of stantienite. *Bull Hist Chem.* 2016;40:86–94.
18. Schaefer J, Stejskal EO. Carbon-13 nuclear magnetic resonance of polymers spinning at the magic angle. *J Am Chem Soc.* 1976;98:1031–2.
19. Lambert JB, Frye JS, Carriveau GW. The structure of oriental lacquer by solid state nuclear magnetic resonance spectroscopy, J. B. Lambert. *Archaeometry.* 1994;33:87–93.
20. Spiker EC, Hatcher PG. The effects of early diagenesis on the chemical and stable carbon isotopic composition of wood. *Geochim Cosmochim Acta.* 1987;51:1385–91.
21. Hatcher PG, Breger IA, Earl WL. Nuclear magnetic resonance studies of ancient buried wood-i observations on the origin of coal to the brown coal stage. *Org Geochem.* 1981;3:49–55.
22. Attalla MI, Serra RG, Vassalo AM, Wilson MA. Structure of ancient buried wood from *Phyllocladus trichomanoides*. *Org Geochem.* 1988;12:235–44.
23. Bardet M, Foray MF, Trần Q-K. High-resolution solid-state CPMAS NMR study of archaeological woods. *Anal Chem.* 2002;74:4386–90.
24. Bardet M, Foray MF, Maron S, Goncalves P, Trần Q-K. Characterization of wood components of Portuguese medieval dugout canoes with high-resolution solid-state NMR. *Carbohydr Polym.* 2004;57:419–24.
25. Pournou A. Deterioration assessment of waterlogged archaeological lignocellulosic material via <sup>13</sup>C CP/MAS NMR. *Archaeometry.* 2008;50:129–41.
26. Bardet M, Gerbaud G, Trần Q-K, Hediger S. Study of Interactions between polyethylene glycol and archaeological wood components by <sup>13</sup>C high-resolution solid-state CP-MAS NMR. *J Arch Sci.* 2007;34:1670–6.
27. Bardet M, Pournou A. Fossil wood from the miocene and oligocene epoch: chemistry and morphology. *Magn Reson Chem.* 2015;53:9–14.
28. Abraham H. *Asphalt and allied substances: their occurrence, modes of production, uses in the arts, and methods of testing*. 4th ed. New York: D. Van Nostrand Co.; 1938.

29. Connan J, Nissenbaum A. The organic geochemistry of the hasbeya asphalt (Lebanon): comparison with asphalts from the Dead Sea area and Iraq. *Org Geochem.* 2004;35:775–89.
30. Michon LC, Netzel DA, Turner TF, Martin D, Planche J-P. A  $^{13}\text{C}$  NMR and DSC study of the amorphous and crystalline phases in asphalts. *Energy Fuel.* 1999;13:602–10.
31. Helms JR, Kong X, Salmon E, Hatcher PG, Schmidt-Rohr K, Mao J. Structural characterization of gilsonite bitumen by advanced nuclear magnetic resonance spectroscopy and ultrahigh resolution mass spectrometry revealing pyrrolic and aromatic rings substituted with aliphatic chains. *Org Geochem.* 2012;44:21–36.
32. Al-Sammerrai F, Al-Sammerrai D, Al-Rawi J. The use of thermogravimetry and NMR spectroscopy in the attempted identification of the source of Babylonian building asphalt. *Thermochim Acta.* 1987;115:181–8.
33. Oudemans TFM, Boon JJ, Botto RE. FTIR and Solid-State  $^{13}\text{C}$  CP/MAS NMR spectroscopy of charred and non-charred solid organic residues preserved in roman Iron age vessels from The Netherlands. *Archaeometry.* 2007;49:571–94.
34. Oudemans TFM. Molecular studies of organic residues preserved in ancient vessels. Ph.D. Dissertation, Faculty of Archaeology, Leiden University, Leiden; 2006.
35. Sherriff BL, Tisdale MA, Sayer BG, Schwarz HP, Knif M. Nuclear magnetic resonance spectroscopic and isotopic analysis of carbonized residues from subarctic Canadian prehistoric pottery. *Archaeometry.* 1995;37:571–94.
36. Styring AK, Manning H, Fraser RA, Wallace M, Jones G, Charles M, Heaton THE, Bogaard A, Evershed RP. The effect of charring and burial on the biochemical composition of cereal grains: investigating the integrity of archaeological plant material. *J Arch Sci.* 2013;40:4767–79.
37. Coe MD. America's first civilization: discovering the olmecs. New York: The Smithsonian Library; 1968.
38. Hosler D, Burkett SL, Tarkanian MJ. Prehistoric polymers: rubber processing in ancient mesamerica. *Science.* 1999;284:1988–91.
39. Lambert JB, Frye JS, Carriveau GW. The structure of oriental lacquer by solid-state nuclear magnetic resonance spectroscopy. *Archaeometry.* 1991;33:87–93.
40. Kvavadze E, Bar-Yosef O, Belfer-Cohen A, Boaretto E, Jakeli N, Matskevich Z, Meshveliani T. 30,000-year-old wild flax fibers. *Science.* 2009;325:1359.
41. Yafa S. Cotton: the biography of a revolutionary fiber. London: Penguin Group; 2005.
42. Adebajo MO, Frost RL. Infrared and  $^{13}\text{C}$  MAS nuclear magnetic resonance spectroscopic study of acetylation of cotton. *Spectrochim Acta A.* 2004;60:449–53.
43. Princi E, Vicini S, Proietto N, Capitani D. Grafting polymerization on cellulose based textiles: a  $^{13}\text{C}$  solid state NMR characterization. *Eur Polym J.* 2005;218:343–52.
44. Taylor RE, French AD, Gamble GR, Himmesbaej DS, Stipanovic RD, Thibodeaux DP, Wakelyn PJ, Dybowski D.  $^1\text{H}$  and  $^{13}\text{C}$  solid-state NMR of *Gossypium barbadense* (Pima) cotton. *J Mol Struct.* 2008;878:177–84.
45. Baias M, Demco DF, Popescu C, Fecete R, Melian C, Blümich B, Möller M. Thermal denaturation of hydrated wool keratin by  $^1\text{H}$  solid state NMR. *J Phys Chem, Part B.* 2009;113:2184–92.
46. Asakura T, Suzuki Y, Nakazawa Y, Holland GP, Yarger JL. Elucidating silk structure using solid-state NMR. *Soft Matter.* 2013;9:11140–50.
47. Creager MS, Jenkins JE, Thagard-Yeamon LA, Brooks AE, Jones JA, Lewis RV, Holland GP, Yarger JL. Solid-state NMR comparison of various spiders' dragline silk fiber. *Biomolecules.* 2010;11:2039–43.
48. Chûiô R, Shimaoka A, Nagaoka K, Kurata A, Inoue M. Primary structure of archeological silk and ancient climate. *Polymer.* 1996;37:3693–6.
49. Chûiô R, Fukutani K, Magoshi Y. Estimation of physical properties of archaeological silk with NMR relaxation time and fluctuation-dissipation theorem in NMR spectroscopy of polymers in solution and in solid state. *Am Chem Soc Symp Ser.* 2002;834:83–91.
50. Bardet M, Gerbaud G, La Pape L, Hediger S, Trân Q-T, Boumlil N. Nuclear magnetic resonance and electron paramagnetic resonance as analytical tools to investigate the structural features of archaeological leathers. *Anal Chem.* 2009;81:1505–11.

51. Capitani D, Di Tullio V, Proiette N. Nuclear magnetic resonance to characterize and monitor cultural heritage. *Prog Nucl Magn Reson Spectrosc.* 2012;64:29–69.
52. Popescu C, Budrugaec P, Wortmann F-J, Miu L, Demco DE, Baias M. Assessment of collagen-based materials that are supports of cultural and historical objects. *Polym Degrad Stab.* 2008;93:976–82.
53. Lambert JB. *Traces of the past.* Cambridge, MA: Helix Books, Perseus Publishing; 1997. p. 148.
54. Aliev AE. Solid-state NMR studies of collagen-based parchments and gelatin. *Biopolymers.* 2005;77:230–45.
55. Odlyha M, Cohen NS, Foster GM, Aliev A, Verdonck E, Grandy D. Dynamic mechanical analysis (DMA),  $^{13}\text{C}$  solid state NMR and micro-thermomechanical studies of historical parchment. *J Thermal Anal Calorimetry.* 2003;71:939–50.
56. Bastone S, Armetta F, Caponetti E. Physicochemical characterization of ancient paper and parchment with solid state nuclear magnetic resonance. In: Fifth European chemistry congress (EuChemS) abstracts, Part 3, P-B1-006. 2014. [http://euchems2014.org/abstract\\_submission.asp](http://euchems2014.org/abstract_submission.asp)
57. Corsaro C, Mallamace D, Łojewska J, Mallamace F, Pietronero L, Missori M. Molecular degradation of ancient documents revealed by  $^1\text{H}$  HR-MAS NMR spectroscopy. *Sci Rep.* 2013;3:2896.
58. Huster D. Solid-state NMR studies of collagen structure and dynamics in isolated fibrils and in biological tissues. *Annu Rep NMR Spectrosc.* 2008;64:127–59.
59. Weber F, Böhme J, Scheidt HA, Gründer W, Rammelt S, Hacker M, Schulz-Siegmund M, Huster D.  $^{31}\text{P}$  and  $^{13}\text{C}$  solid-state NMR spectroscopy to study collagen synthesis and biomineralization in polymer-based bone implants. *NMR Med.* 2012;3:464–75.
60. Mroue KH, MacKinnon N, Xu J, Zhu P, McNerny E, Kohn DH, Morris MD, Ramamoorthy A. High-resolution structural insights into bone: a solid-state NMR relaxation study utilizing paramagnetic doping. *J Phys Chem B.* 2012;116:11656–61.
61. Duer MJ. The contribution of solid-state NMR spectroscopy to understanding biomineralization: atomic and molecular structure of bone. *J Magn Reson.* 2015;253:98–110.
62. Lee AP, Klinowski J, Maseglia EA. Application of nuclear magnetic resonance spectroscopy to bone diagenesis. *J Archaeol Sci.* 1995;22:257–62.
63. Alfano D, Alburnia AR, Motta O, Proto A. Detection of diagenetic alterations by spectroscopic analysis on archaeological bones from the necropolis of poseidonia (Paestum): a case study. *J Cult Herit.* 2009;10:509–13.
64. Saless K, Urzel V, Dufour E, Castex D, Bruzek J, Dufour EJ. Validation of bone apatite purification protocols for stable isotope analysis in bioarchaeology by solid-state nuclear magnetic resonance spectroscopy, Abstracts of the 82nd annual meeting of the American association of physical anthropologists. *Am J Phys Anthropol.* 2013;150(S56):239.
65. Turcu RV, Kelemen RVF, Popescu O, Simon S. Solid state NMR preliminary study on archaeological bones. *Studia Univ Babeş-Bolyai Physica.* 2012;57(2):61–8.
66. Blümich B. Magnetic resonance imaging and portable NMR in archaeological sciences. In: *Modern Magnetic Resonance.* 2nd ed. Switzerland: Springer International Publishing; 2017.
67. Kehlet C, Kuvvetli F, Catalano A, Dittmer J. Solid-state NMR for the study of Asger Jom's paintings. *Microchem J.* 2016;125:308–16.